

# A Quantum Mesoscopic RC Circuit Realized in a 2D Electron Gas

J Gabelli <sup>a,1</sup>, J.M. Berroir <sup>a</sup>, G. Fève <sup>a</sup>, B. Plaçais <sup>a</sup>, Y. Jin <sup>b</sup>, B. Etienne, <sup>b</sup>, and D.C. Glattli <sup>c,a</sup>

<sup>a</sup>Lab. Pierre Aigrain, Département de Physique, Ecole Normale Supérieure, F-75231 Paris, France

<sup>b</sup>Lab. Photonique et Nanostructures, route de Nozay, 91 Marcoussis, France

<sup>c</sup>SPEC, CEA Saclay, F-91191 Gif-sur-Yvette, France

## Abstract

The quantum resistance and capacitance of a mesoscopic RC-circuit made of a small dot connected to a lead by a QPC realized in a 2DEG are measured for the first time. Contrary to what can be naively expected, in the coherent regime the resistance is not given by the Landauer formula but is nearly constant and is found to be close to half the resistance according to Buttiker's ac quantum scattering theory.

*Key words:* quantum transport, mesoscopic phenomena, capacitance, high frequency

*PACS:* 72.10.Bg, 72.30.+q

We present measurements of the a.c. conductance of a mesoscopic RC circuit. The capacitor is made of a macroscopic metallic electrode on top of a 2DEG sub-micrometer dot defining the second electrode. The resistor is a Quantum Point Contact (QPC) connecting the dot to a wide 2DEG macroscopic reservoir, as schematically shown in Fig. 1(a). We address the mesoscopic regime where electrons emitted from the reservoir to the dot are backscattered without loss of coherence. In this new regime, we have checked for the first time the counter-intuitive prediction made in Ref.[1] that the resistance, also called charge relaxation resistance, is *no longer* given by the Landauer formula but remains *constant* and ideally equal to  $h/2e^2$  when the QPC transmission is varied.

According to [1], in the coherent regime and when a single mode is transmitted, the mesoscopic capacitor is

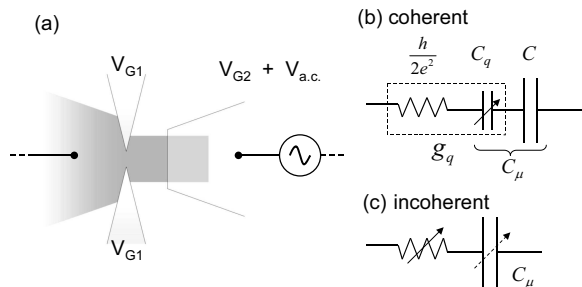


Fig. 1. Mesoscopic capacitor connected to a 2D lead by a QPC and coherent and incoherent regime equivalent circuit.

represented by the equivalent circuit of Fig. 1(b). The electrical capacitance  $C$  is in series with the quantum admittance  $g_q(\omega)$  relating the ac current flowing to the QPC to the ac internal potential of the dot:

$$g_q(\omega) = \frac{1}{\frac{h}{2e^2} + \frac{1}{-i\omega C_q}} \quad (1)$$

<sup>1</sup> Corresponding author. E-mail: gabelli@lpa.ens.fr

It represents the series addition of the quantum capacitance  $C_q = e^2 \frac{dN}{d\epsilon}$  associated with the local density of state  $\frac{dN}{d\epsilon}$  of the mode propagating in the dot with a *constant* contact resistance  $h/2e^2$ . The striking effect of phase coherence is that the transmission probability  $D$  only affects the quantum capacitance but not the resistance. Indeed, an electron emitted from the reservoir returns with unit probability in the same (unique) reservoir. In the incoherent regime, Fig 1(c), both resistance and quantum capacitance vary with transmission. The dot forms a second reservoir and the electrochemical capacitance  $C_\mu = \frac{CC_q}{C+C_q}$  is in series with QPC resistance whose conductance is now given by the Landauer formula.

Several samples have been measured at low temperature, down to 30mK, which show similar features. We present here measurements on two samples made with 2D electron gas defined in the same high mobility GaAsAl/GaAs heterojunction, with nominal density  $n_s = 1.7 \times 10^{15} \text{m}^{-2}$  and mobility  $\mu = 260 \text{V.m}^{-2} \text{s}^{-1}$ . Their geometry is similar to that of Fig. 1(a). A pair of QPC gates, d.c. voltage  $V_{G_1}$ , controls the transmission and a gate  $G_2$  defines the counter-electrode, capacitance  $C_0$ , to apply both microwave voltage  $V_{ac}$  and dc voltage  $V_{G_2}$ . The dots are patterned by shallow etching. Their targeted lithographic size is about 1000nm (1500nm) long for sample I and II respectively and 1000nm wide. To estimate the real size one has however to subtract about 300nm to each dimensions to take into account edge depletion. The coupling capacitor  $C_0$ , part of the total electrical capacitance dot  $C$ , overlaps partly the dot over an area  $\simeq 0.5 \mu\text{m}^2$ .  $C_0$  being in the sub-fF range, GHz frequencies are used such that  $1/C_0\omega$  is about ten times  $h/2e^2$ . Higher frequencies are not suitable for  $\hbar\omega$ ,  $\simeq 50\text{mK}$  at 1 GHz, would become much larger than  $k_B T$  and comparable to other energy scales, complicating the analysis. To perform measurements of the complex mesoscopic capacitor admittance the rf source of a monochromatic radio-frequency synthesizer is attenuated by 80dB and sent to  $G_2$ . The current induced in the mesoscopic capacitor is detected by measuring the ac voltage on a 50 Ohms characteristic impedance coaxial line in series with the ohmic contact to which the electron reservoir is connected. The signal is sent to an ultra low noise cryogenic amplifier followed by room temperature amplifiers. Two mixers using the reference source signal and a  $90^\circ$  phase shifter allow to simultaneously detect

real  $Re(G)$  and imaginary  $Im(G)$  parts of the admittance  $G = \frac{-i\omega C}{-i\omega C + g_q(\omega)}$  [2]. In the limit of small resistance compared to  $1/C_\mu\omega$ :

$$G \simeq -i\omega C_\mu + R_q(\omega C_\mu)^2 + \dots \quad (2)$$

The imaginary part measures the electrochemical capacitance and the real part contains information on the charge relaxation resistance  $R_q$  expected constant and  $\simeq h/2e^2$  for one orbital mode in the coherent regime at  $T = 0$ . Finally, the detection bandwidth is 1-2 GHz and the  $\simeq 12\text{K}$  amplifier noise temperature allows to detect  $\simeq 4\text{pA}$  in one second. The ac current range never exceeds  $\simeq 80\text{pA}$  such that the linear response is ensured. To protect the sample from electromagnetic environment noise the attenuators are placed at low temperature and two cryogenic rf circulators in series, one at the lowest temperature, are inserted before the first amplifier.

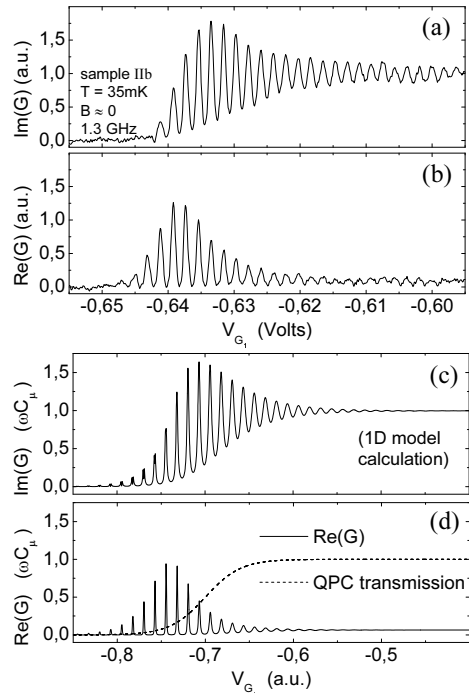


Fig. 2. imaginary (a) and real (b) admittance versus QPC voltage measured in sample II. Only, the last orbital mode before pinch-off is probed here.  $Im(G)$  is normalized to 1 at full transmission. In (c) and (d): admittance calculated for a non-interacting 1D model. (d) dashed curve: QPC transmission used for the calculation.

We now present the experimental results. We emphasize that the present approach differs from previous capacitance measurements where, for spectroscopic purpose, the dot-reservoir coupling was weak and the regime was incoherent [3]. Also, in these experiments, the charge relaxation resistance was not measured. Fig. 2(a)-(b) display  $\text{Im}(G)$  and  $\text{Re}(G)$  versus the QPC gate voltage obtained for sample II at 35mK,  $B \simeq 0\text{T}$  and 1.3GHz. From left to right we can distinguish two regimes. Starting from the pinch-off regime fast growing peaks in both  $\text{Im}(G)$  and  $\text{Re}(G)$  are observed. Then  $\text{Im}(G)$  reaches a maximum and a second regime occurs where  $\text{Im}(G)$  oscillates nearly symmetrically around a plateau and the oscillation amplitudes decrease smoothly. Simultaneously peaks in  $\text{Re}(G)$  quickly disappear to vanish in the noise. To get better insight, it is interesting to compare with the results expected from [1] for a simplified 1D model with one mode. The zero temperature quantum capacitance is:

$$C_q = \frac{e^2}{\Delta} \frac{1 - r^2}{1 - 2r \cos 2\pi \frac{\varepsilon}{\Delta} + r^2} \quad (3)$$

where  $r$ ,  $r^2 = 1 - D$ , is the reflection amplitude modulus,  $\Delta$  the energy level spacing and  $\varepsilon$  the energy. The capacitance averaged over energy coincides with the  $r = 0$  value  $e^2/\Delta$  expected for the density of state in 1D. When reflection increases  $C_q$  shows growing oscillations between two extrema  $\frac{e^2}{\Delta} \frac{1+r}{1-r}$  and  $\frac{e^2}{\Delta} \frac{1-r}{1+r}$ . For strong reflection it displays resonant Lorentzian peaks  $\frac{e^2}{\Delta} \frac{1+r}{1-r} \frac{1}{1+(2\delta\varepsilon/\hbar\Gamma)^2}$ , with  $\hbar\Gamma = D\Delta$  and  $\delta\varepsilon = \varepsilon - \varepsilon_{res}$  denotes the energy departure from a resonant dot level  $\varepsilon_{res}$  at the Fermi energy. At finite temperature, the conductance  $g_q(\omega)$  formed by the contact resistance  $h/2e^2$  and the quantum capacitance in series becomes:

$$g_q(\omega) = \int d\varepsilon \left( -\frac{\partial f}{\partial \varepsilon} \right) \frac{1}{h/2e^2 + 1/(-i\omega C_q)} \quad (4)$$

In the large transmission regime ( $r \rightarrow 0$ ) capacitance oscillations are reduced by the visibility factor  $(2\pi^2 k_B T / \Delta) / \sinh(2\pi^2 k_B T / \Delta)$ . In the weak transmission regime, when  $\hbar\Gamma \ll k_B T$ , the capacitance peaks are thermally broaden with  $C_q \simeq \frac{e^2}{4k_B T \cosh(\delta\varepsilon/2k_B T)^2}$  and the resistance is *no longer constant*.  $1/R_q \simeq D \frac{e^2}{h} \frac{\Delta}{4k_B T \cosh(\delta\varepsilon/2k_B T)^2}$  is reminiscent of the thermally broaden resonant tunneling conductance formula: the Landauer formula is recovered. Figs. 2(c-d) show the calculated  $\text{Im}(G)$ ,  $\text{Re}(G)$  with  $\Delta \ll e^2/C$ .  $V_{G1}$  is assumed to vary both the 1D dot potential and the

transmission  $D$  (dashed line in Fig. 2(d)). The similarity with the experimental conductance traces is striking. It is important to note that in a real system the weak transmission regime is accompanied by Coulomb blockade effects not taken into account in this simple model. A  $T = 0$  an elastic co-tunneling approach, valid at weak transmission, shows no qualitative change except in the energy scale which has to include the charging energy ( $\Delta$  replaced by  $e^2/C_\mu$ ). At present, for finite temperature and large transmission, no available model exists which could include both charge relaxation resistance and quantum capacitance.

Low temperature conductance traces for an other sample (sample I) at different frequency (1.085 GHz) show similar features, Fig. 3(a). In Fig. 3(b) we have numerically calculated the reciprocal of the admittance to display the real and imaginary part of the impedance to study the weak reflection regime. Capacitances and resistance being in series, one expects that the charge relaxation resistance and the reciprocal of the electrochemical capacitance separate into the real and imaginary part respectively. While the capacitive part shows growing oscillations when the transmission is reduced with QPC gate, we find a large region ( $V_{G1} > -0.76\text{Volts}$ ) where the resistance *remains constant*. For lower  $V_{G1}$  however both resistance and capacitance strongly vary. The separation between the two regimes is best depicted on the Nyquist diagram where  $\text{Im}(G)$  is plotted against  $\text{Re}(G)$ . Constant resistance variations are expected to follow a circle centered on the real axis while constant capacitance variations follow a circle centered on the imaginary axis. Data are shown in Fig. 3(c) and results of the previous calculation are shown in Fig. 3(d) for qualitative comparison. The capacitance oscillations of the weak reflection regime follow the dashed line circle demonstrating again a constant resistance regime. On the other hand, at weak transmission, in the thermally broaden regime, both capacitance and resistance vary and their resonant peaks show a series of lobes which fan out. At capacitance minima, as  $k_B T$  is lower than the energy separation, the thermal has negligible effect and the loci of the minima are shown to still follow the constant resistance line. This shows that the *constant resistance* prediction is well verified even in the regime of *weak transmission*.

Finally, it is interesting to estimate the absolute value of the constant contact resistance  $R_q$ . Measuring

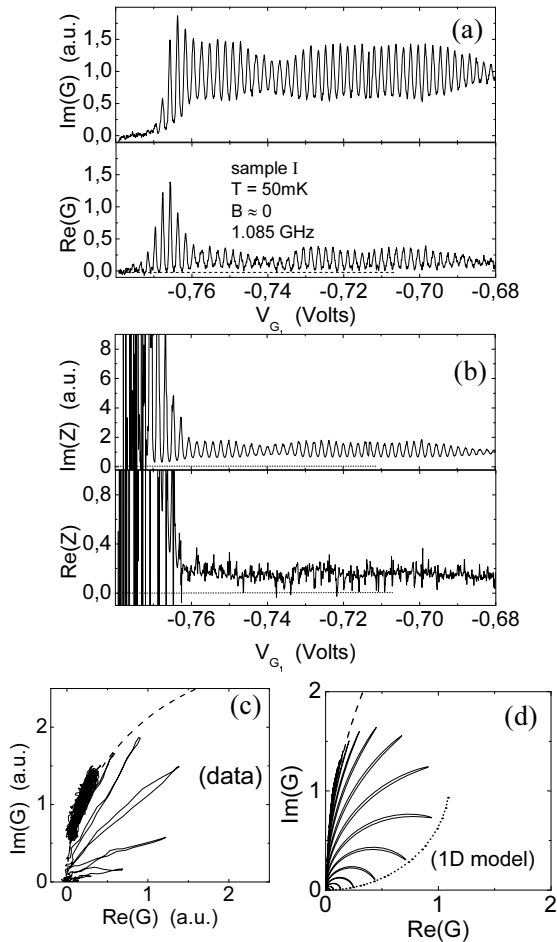


Fig. 3. imaginary and real admittance observed in sample I (a) and (b) numerically calculated corresponding impedance. The Nyquist representation (c) shows that except for the first thermally broaden peaks, the admittance variation follow a constant resistance circle. (d) Nyquist plot of the 1D model. Dashed (dotted) curves correspond to circle with constant resistance (capacitance) variations.

the absolute value of the admittance is a possibility. However at GHz frequencies calibration of the whole detection chain and of the coupling to the sample is difficult and accuracy is not better than 3dB. Comparing real and imaginary part is another option. In the weak reflection regime, the signal phase is  $\simeq 1/R_q C_\mu \omega$ . It can be known within one degree accuracy. Thus it remains to determine  $C_\mu$  to estimate  $R_q$ . To do that we choose the clean situation of high magnetic field where edge states form. We concentrate on the last transmitted  $\nu = 1$  edge channel while  $\nu \simeq 4$  in the 2D reservoir.

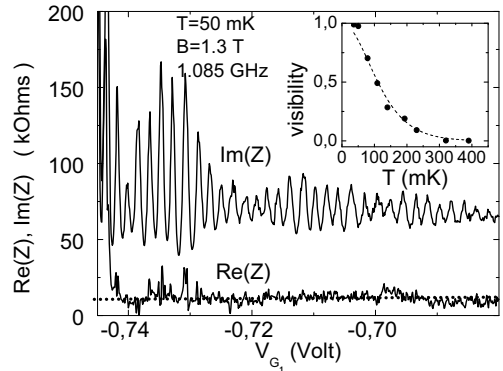


Fig. 4. Impedance of sample I in the QHE regime. The inset shows the visibility of the capacitance variations versus temperature (closed circles). The dashed line fit allows to extract  $C_\mu$  so calibrating the impedance scale used.

Here spin degeneracy is lifted and  $R_q$  is expected to be  $h/2e^2$ . The 1D type density of state makes  $\Delta$  and  $e^2/C$  contributing nearly equally to the charging energy  $e^2/C_\mu$ . To determine  $e^2/C_\mu$  we used the temperature dependence of the visibility of the capacitance oscillations at large transmission which should vary as  $(2\pi^2 k_B T / \Delta^*) / \sinh(2\pi^2 k_B T / \Delta^*)$  (Fig. (4), inset). Identifying  $\Delta^* \simeq 0.9\text{K}$  to  $e^2/C_\mu$ , we have plotted the measured real and imaginary part of the impedance. We estimate  $R_q = 10.5 \pm 3\text{kOhms}$ . Probably, in the weak reflection regime,  $\Delta < \Delta^* < e^2/C_\mu$  [4] and  $R_q$  may be underestimated, but it is definitely lower than  $h/e^2$ . In conclusion we have shown for the first time that the charge relaxation resistance remains constant for a coherent mesoscopic capacitor when transmission varies. Further data are needed to accurately identify  $R_q$  to  $h/2e^2$ .

We acknowledge useful discussions with M. Büttiker, S. Nigg, Th. Jolicoeur, X. Waintal.

## References

- [1] M. Büttiker, A. Prêtre, and H. Thomas, Phys. Rev. Lett. **70**, 4114 (1993); A. Prêtre, H. Thomas, and M. Büttiker, Phys. Rev. B. **54**, 8130 (1996).
- [2] The conductance actually measured is reduced by the coupling factor  $C_0/C$ .
- [3] R. C. Ashoori et al. Phys. Rev. Lett. **68**, 3088 (1992); Phys. Rev. Lett. **71**, 613 (1992);
- [4] L.I. Glazman, I.L. Aleiner, Phys. Rev. B **57**, 9608 (1998).